DE GRUYTER

Chemical Papers 70 (7) 960–972 (2016)
DOI: 10.1515/chempap-2016-0032

ORIGINAL PAPER

Role of polydimethylsiloxane in properties of ternary materials based on polyimides containing zeolite Y

Merve Biçen, Sevim Karataş, Nilhan Kayaman-Apohan*, Atilla Güngör

Department of Chemistry, Marmara University, 34722 Göztepe/Istanbul, Turkey

Received 25 August 2015; Revised 6 December 2015; Accepted 16 December 2015

Mixed matrix materials, containing poly(dimethylsiloxane), phosphine oxide-based polyimide, and zeolite Y were prepared by means of blending hybridisation. The thermal stability of the materials and the hydrophobic properties were enhanced. The decrease in the glass transition temperature of the materials with the increase in poly(dimethylsiloxane) content supported the polymer-chain flexibility. The pristine polyimide and the zeolite-filled polyimide exhibited the highest transparency. Fourier transform infrared (FTIR) spectroscopy confirmed that the increase in the amount of the lowest molecular mass poly(dimethylsiloxane) ingredient indicated strong alkyl and Si—O—Si stretching modes, whilst the alkyl and Si—O—Si stretching intensity decreased in the presence of the highest amount of and the highest molecular mass poly(dimethylsiloxane). The hydrophobic poly(dimethylsiloxane) moiety created an inverse relationship between the porosity of the materials (surface roughness) and the hydrophilicity. The nanocrystallite domain, identified by X-ray diffraction analysis (XRD) and possessing an exotherm crystallisation peak, occurred in the lowest amount of poly(dimethylsiloxane) with the highest molecular mass-based hybrid material. The nanocrystallite enhanced the storage modulus as determined by the dynamic mechanical analyser (DMA). The nanocrystalline formation resulted in a slight increase in the alkyl stretching and the Si—O—Si stretching of the lowest amount of and the highest molecular mass poly(dimethylsiloxane)-containing material over those of the lowest molecular mass poly(dimethylsiloxane) in the same amounts of material involved.

Keywords: phosphors, porous materials, polymeric composites, morphology, nanocrystalline

Introduction

Aromatic polyimides (PIs) are important components in the electronics, microelectronics, and aircraft industries, as well as of membranes, since they exhibit high thermal and mechanical strength, good optical properties, and chemical resistance as detailed by Hennepe et al. (1987). Freeman (1999) found that the performance of PIs might be further improved with the zeolite. Porous and/or non-porous materials might act as hosts within a host–guest system. Zeolites possessing Al—O—Si and Si—O—Si bonds are porous aluminosilicates. Organic molecules can be incorporated within the zeolite pores, as described by Steed and Atwood (2009). In this way, the organic–inorganic moiety represents a host–guest hybrid. Kickelbick (2003) showed that polymers could be entrapped in the host channels, these being of a limited size, not only by diffusion into the pores but also by in situ polymerisation in the porous material. A zeolite-filled material in the presence of glassy polymers can cause voids due to the poor adhesion between the polymer and the zeolite surface. To resolve this issue, some coupling agents (i.e. (3-aminopropyl)trimethoxysilane) could be used. The addition of inorganic fillers to a polymer increases the tensile modulus and tensile strength but reduces the elongation at break, hence the material becomes brittle as recorded by Alam et al. (2007).

*Corresponding author, e-mail: napohan@marmara.edu.tr

Nakata et al. (1993) and Kricheldorf (1996) showed that poly(dimethylsiloxane) (PDMS) acts as an important inorganic polymer, as it is flexible and exhibits such properties as good thermal stability and high hydrophobicity. A novel ternary system involving PDMS, PI, and zeolite was prepared in the present study. The purpose of the PDMS addition was to determine how the tensile properties of the mixed matrix materials (MMMs) were influenced. Two different molecular mass PDMS materials in two different, limited amounts (3.2 mass % or 5.2 mass %) for a proper blend were used so as to discern the difference in the tensile properties of the ternary system. The improved mechanical properties resulting from increasing the amount of PDMS in MMMs had been anticipated. However, 5.2 mass % of the PDMS ingredient adversely affected the tensile properties. The thermal stability of the materials was good. The MMMs exhibited good hydrophobicity due to the introduction of the PDMS. Although a linear relationship between the porosity of the material and the hydrophilicity was expected, the bonding type of a large amount of hydrophobic PDMS content onto zeolite-filled polyimide adversely affected the porosity–hydrophilicity property. The 5.2 mass % of PDMS (3200 g mol^{-1}) could surround the zeolite-containing polyimide through non-covalent interaction rather than polymerisation in the zeolite pores. The polymerisation outside the zeolite pores could be explained by the observation of a slight decrease in the alkyl and Si—O—Si stretching in the 5.2 mass % of PDMS (3200 g mol^{-1})-based material in comparison with 3.2 mass % of PDMS (3200 g mol^{-1}). The lowest molecular mass PDMS (1000 g mol^{-1}) with the highest amount (5.2 mass %) led to the increase in the intensity of the alkyl and Si—O—Si stretching. In addition, 3200 g mol^{-1} and 5.2 mass % of PDMS decreased the CH_3—Si ^{1}H NMR peak intensity compared with that of 3.2 mass % PDMS (3200 g mol^{-1}). A decrease in the glass transition temperature with an increase in the PDMS content was also observed. The different molecular mass PDMS in a high concentration represented an important feature especially in the mechanical and morphological properties of the ternary mixed-matrix materials. The nanocrystallite in the lowest amount (3.2 mass %) and the highest molecular mass PDMS (3200 g mol^{-1})-based material improved the storage modulus (E') except for that of the zeolite-filled polyimide.

Experimental

Benzophenone-3,3′,4,4′-tetracarboxylic dianhydride (BTDA, purified by sublimation, 96 %), 4,4′-oxydianiline (ODA, 99 %), phenylphosphonic dichloride (98 %), 1-bromo-4-fluorobenzene (99 %), Mg powder (99.9 %), anhydrous potassium carbonate (K_2CO_3, 99.9 %), 3-aminophenol, and 3-(aminopropyl) trimethoxysilane (97 %) were provided by Aldrich, Turkey. N-methyl-2-pyrrolidone (NMP), dimethylacetamide (DMAc) obtained from Merck (Turkey) and tetrahydrofuran (THF) obtained from Fluka (Turkey) were freshly distilled. Zeolite Y ($n(SiO_2) : n(Al_2O_3)$, 5 : 1) was purchased from Alfa Aesar, UK. PDMS (amine-terminated, $M_n = 3200$ and $M_n = 1000$) was obtained from Koç University, Turkey.

The FTIR spectra were recorded on a Perkin–Elmer (Turkey) Spectrum 100 ATR FTIR spectrophotometer. The NMR spectra were recorded on a Varian 600 MHz spectrometer (Turkey). The solvent was DMSO-d_6. Thermogravimetric analyses (TGA) were performed using a Perkin–Elmer thermogravimetric analyser Pyris 1 TGA model (Turkey) running from 30 ℃ to 800 ℃ with a heating rate of 20 ℃ min^{-1} under atmospheric air. For the TGA measurements, the initial mass of samples was 13–18 mg. Differential scanning calorimetry (DSC) was performed using a Perkin–Elmer Diamond DSC apparatus (Turkey) under nitrogen flow at a heating rate of 15 ℃ min^{-1} from ambient temperature to 400 ℃. Glass transitions were determined from the second run of DSC analysis. The mass of samples was in the range of 10–15 mg. The mechanical properties were determined on a materials test machine Zwick/Roell model (Turkey) at ambient temperature using compressed air. The specimen dimensions were 0.04–0.1 mm in thickness and 10–15 mm in width. The error range for tensile measurements was ± 0.1–1. The initial length of the samples was 20 mm and the stretching rate was 5 mm min^{-1}. Dynamic mechanical analysis (storage modulus and tanδ) was performed using a Netzsch DMA 242C model (Turkey) under a liquid nitrogen atmosphere in the temperature range between 75 ℃ and 270 ℃ with a heating rate of 10 K min^{-1} for PDMS-containing materials. The more sensitive measurement was performed in the presence of zeolite-filled polyimide (heating rate: 3 K min^{-1}). The width of the samples was 6.4 mm, the maximal dynamic force was 0.5 N and the maximal amplitude was 10 μm. The frequency selected was 1 Hz. The contact angles were measured using a Kruss (Turkey) Easy Drop DSA-2 tensiometer. The scanning electron microscopy (SEM) imaging was performed on a SUPRA 35VP, LEO model (Turkey). The particle size analyses of unmodified and modified zeolite Y were performed on a Brookhaven Particle Size Analyser 90 Plus (Turkey) using zeolites in deionised water as suspension at ambient temperature. The wavelength was 659 nm. The X-ray diffraction analyses of PI–zeolite–PDMS materials were performed using a Rigaku/Max-Ultima+/PC XRD (Turkey), 2θ of which was in the range of 0–70°. "λ" was 1.54 Å (CuK_α). The paste was used for the sample preparation prior to XRD analysis. The clear peaks representing zeolite Y were observed in 3.2 mass % of PDMS (3200 g mol^{-1})-based material. The XS (in Å),

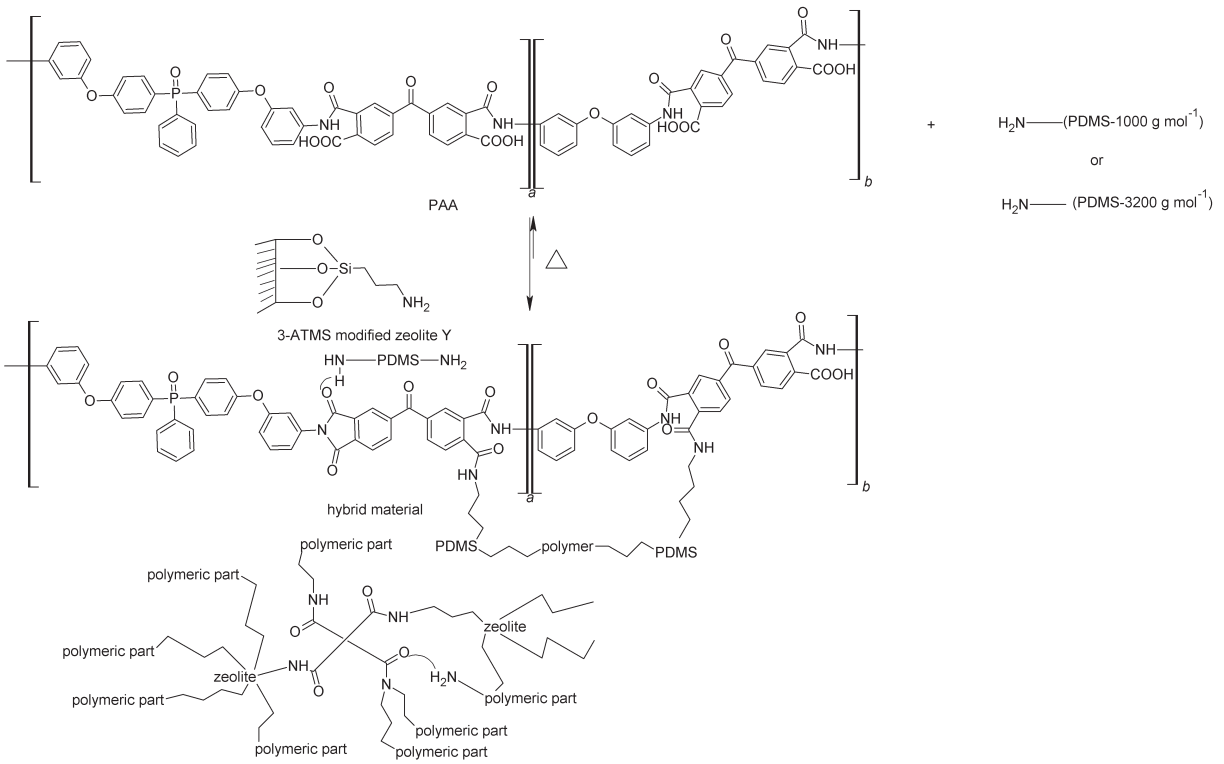

Fig. 1. PI–zeolite–PDMS hybrid material.

crystallite size obtained on the XRD equipment and the calculated crystallite size (in Å) from the Scherrer equation (Eq. (1)) were compared.

$$D_{\mathrm{p}} = \frac{K\lambda}{b\cos\theta} \tag{1}$$

where D_{p} represents the average crystallite size (diameter), b is the line-broadening in radians (1 radian = 57.296°), θ the Bragg angle, λ the X-ray wavelength, and K the constant between 0.9 and 1.

Bis[4-(3-aminophenoxy)phenyl]phenylphosphine oxide (*m*-BAPPO) was synthesised as described by Güngör et al. (1991). A copolyamic acid solution (PAA) was prepared in NMP by allowing ODA, *m*-BAPPO to react with an equimolar amount of BTDA. The solid concentration was 20 mass %. The reaction mixture was stirred at ambient temperature to obtain a viscous and clear PAA solution. For the zeolite modification, toluene and zeolite were transferred into a flask equipped with a condenser and 3-APTMS was added drop-wise. The reaction was maintained at 110 ℃ under N_2 atmosphere. After purification, the product was dried under vacuum at 80 ℃. To obtain the MMMs, 1 mass % of the modified zeolite Y was added to the PAA (10 g) solution and stirred continuously until a clear solution was observed. Then, 3.2 mass %, or 5.2 mass % of PDMS ($M_{\mathrm{n}} = 3200$ g mol^{-1}) were added drop-wise to the PAA–zeolite solution. After thorough stirring, the hybrid solutions were poured onto Teflon® plates. Thermal imidisation was carried out step-wise at 100 ℃, 200 ℃, and 300 ℃ for 1 h at each temperature. After imidisation, the hybrid films were removed from the plates. The same procedures were conducted using 3.2 massa % of, or 5.2 mass % of PDMS ($M_{\mathrm{n}} = 1000$ g mol^{-1}) (Fig. 1).

Results and discussion

Structure characterisation

The FTIR (Fig. 2a) broad peaks between 3250 cm^{-1} and 3750 cm^{-1} ascribed to the –OH stretching of unmodified zeolite Y disappeared with the modification (Fig. 2b). The surface modification of zeolite Y with the treatment of 3-APTMS was successful, taking into consideration both the FTIR spectra (Fig. 2) and the particle size analyses (Fig. 3). The effective diameter depending on the volume calculation was determined as 1.22 μm and the mean diameter depending on the surface area was 1.00 μm in the absence of modification (Fig. 3a). On the other hand, the effective diameter was 2.74 μm and the mean diameter was determined as 2.05 μm for the modified zeolite Y (Fig. 3b). The FTIR (Fig. 4) peaks of the imide at 1776 cm^{-1} (C═O symmetric stretching), 1720 cm^{-1} (C═O asymmetric stretching), and 1378 cm^{-1} (C—N stretching) confirmed the expected MMMs, when compared with the results reported by Zuo et al. (1998). The peak at 3400 cm^{-1} (N—H stretching of alkoxysilane, Fig. 4, spectrum A) disap-

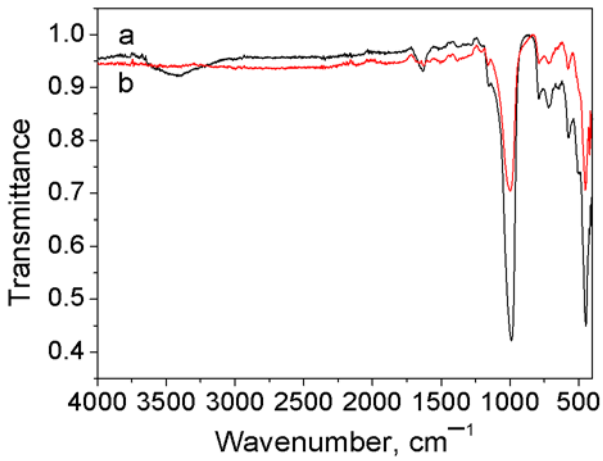

Fig. 2. FTIR spectra of unmodified (a) and modified (b) zeolite Y.

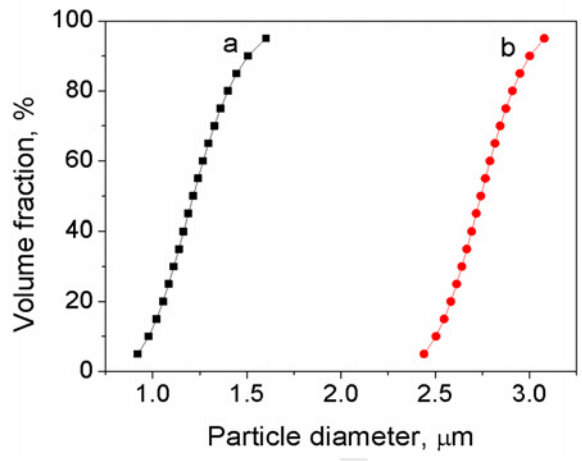

Fig. 3. Particle diameter analyses of unmodified (d(50 vol. %) = 1.22 μm) (a) and modified (d(50 vol. %) = 2.74 μm) (b) zeolite Y.

peared, as a result of the reaction between the modified zeolite and the polyimide (Fig. 4, spectrum B). The peaks related to the zeolite (Figs. 2 and 4, spectrum B) were at 995 cm^{-1} (asymmetric stretching of external linkages), 792 cm^{-1} (symmetric stretching of external linkages), 577 cm^{-1} (double ring external linkage peak close to the result of Sang et al. (2006)), and 451 cm^{-1} (T—O bending; T: Si or Al in zeolite, the peak close to Sang et al. (2006) finding). The presence of PDMS was confirmed by Si—alkyl (807 cm^{-1}) and Si—O—Si (1100 cm^{-1}) stretching modes (Fig. 4, spectra C–F). The alkyl stretching at 2960 cm^{-1} and the Si—O—Si stretching at 1100 cm^{-1} intensity increased with an increase in PDMS (1000 g mol^{-1}) amount (Fig. 4, spectra C and D), while the alkyl and Si—O—Si stretching intensities decreased with an increase in PDMS (3200 g mol^{-1}) (Fig. 4, spectra E and F). Furthermore, the alkyl stretching and Si—O—Si stretching intensities increased slightly with an increase in molecular mass (from 1000 g mol^{-1} to 3200 g mol^{-1}) of 3.2 mass % PDMS (Fig. 4, spectra C and E).

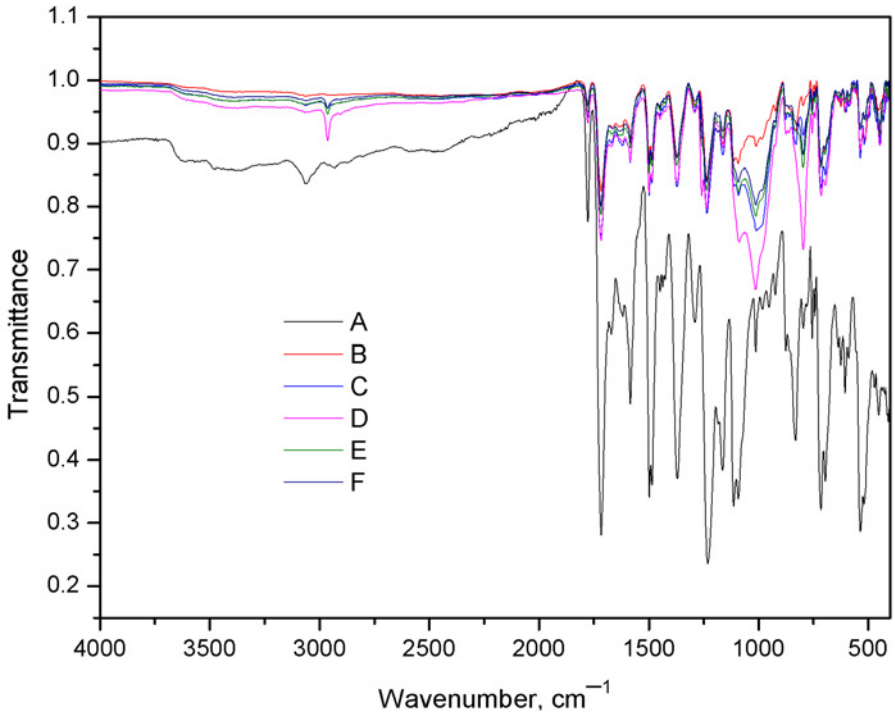

Fig. 4. FTIR spectra of materials: PI (A), PI–zeolite (B), PI–zeolite–3.2 mass % PDMS (1000 g mol^{-1}) (C) PI–zeolite–5.2 mass % PDMS (1000 g mol^{-1}) (D), PI–zeolite–3.2 % PDMS (3200 g mol^{-1}) (E), and PI–zeolite–5.2 % PDMS (3200 g mol^{-1}) (F).

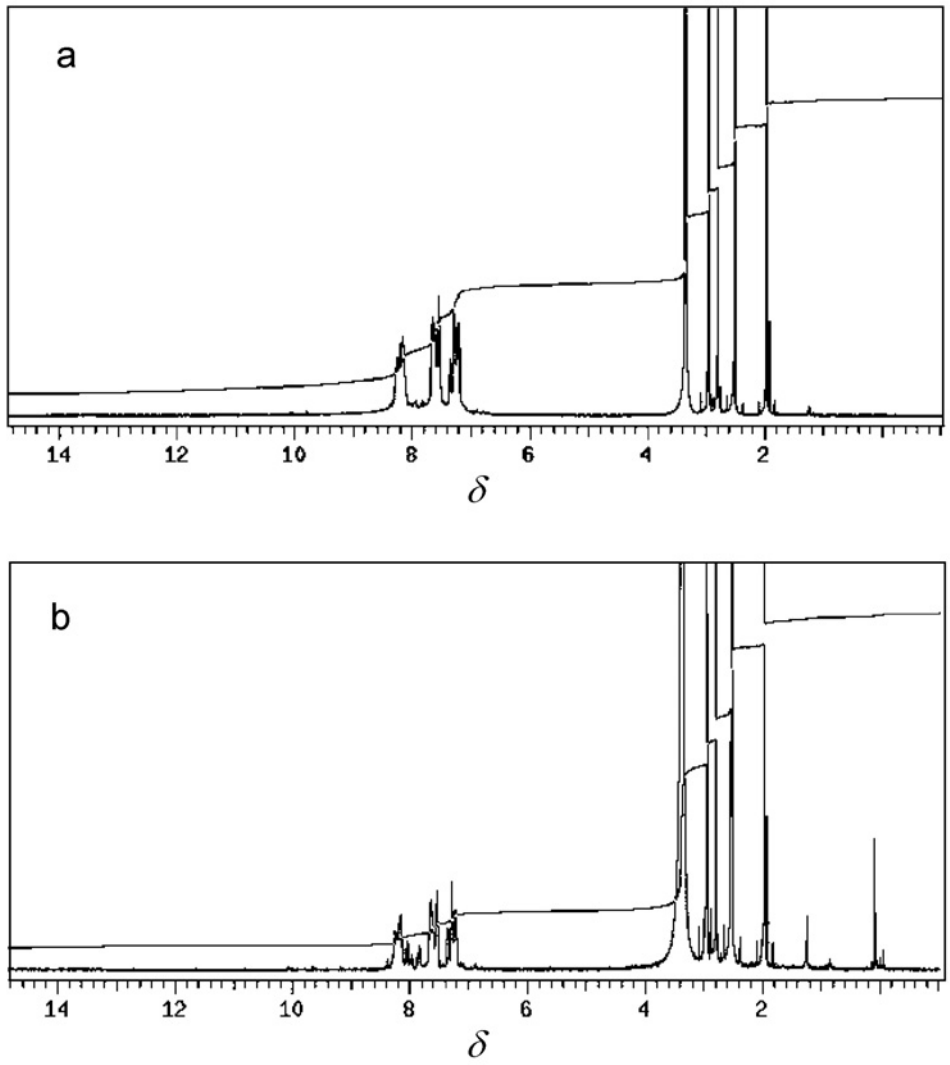

Fig. 5. ^{1}H NMR spectrum of PI–zeolite (a) and PI–zeolite–3.2 mass % PDMS (3200 g mol^{-1}) (b).

^{1}H-NMR peak intensities in the aromatic region (δ = 7–9, Fig. 5a) decreased with the introduction of the PDMS (Fig. 5b).

The ^{1}H NMR intensities in the δ range from –0.10 to 0.5 attributed to CH_3—Si protons decreased with an increase in molecular mass of 5.2 mass % (Fig. 6). The NMR intensity decline of the CH_3—Si protons supported the decrease observed in the FTIR alkyl stretching with the increase in molecular mass in 5.2 mass % PDMS (Fig. 4, spectra E and F). The aromatic field protons of the PI–zeolite peaks intensity increased with an increase in molecular mass of 5.2 mass % PDMS (Fig. 6). In 3.2 mass % PDMS (the lowest amount) with molecular mass of 3200 g mol^{-1} (Fig. 5b), the CH_3—Si intensity was largely the same as with 5.2 mass % PDMS (1000 g mol^{-1}) (Fig. 6a). On the other hand, the intensity of aromatic protons in 3.2 mass % PDMS (3200 g mol^{-1})-containing material (Fig. 5b) was greater than that containing 5.2 mass % PDMS (1000 g mol^{-1}) (Fig. 6a).

Morphological, physical, and hydrophobicity properties

The amino groups of PDMS-(1000 g mol^{-1}) in either 3.2 mass % or 5.2 mass % react with the polyamic acid–zeolite filling the pores, however the PDMS with molecular mass of 3200 g mol^{-1} (5.2 mass %) reacts physically with the zeolite, being adsorbed onto the zeolite surface. The volume fraction of the filler, φ_{zeolite}, determined using Eq. (2), as proposed by Guth (1945), confirms this finding since the $\varphi_{\text{zeolite}} = 0.31$ starts to decrease on the addition of 3.2 mass % PDMS (1000 g mol^{-1}) and 5.2 mass % PDMS (1000 g mol^{-1}) to 0.11, and 0.05, respectively (Table 1).

$$E = E_{\text{m}}\left(1 + 2.5\varphi + 14.1\varphi^2\right) \qquad (2)$$

where E is the modulus of the filled polymer, E_{m} the modulus of the unfilled matrix (PI), and φ is the volume fraction of the filler.

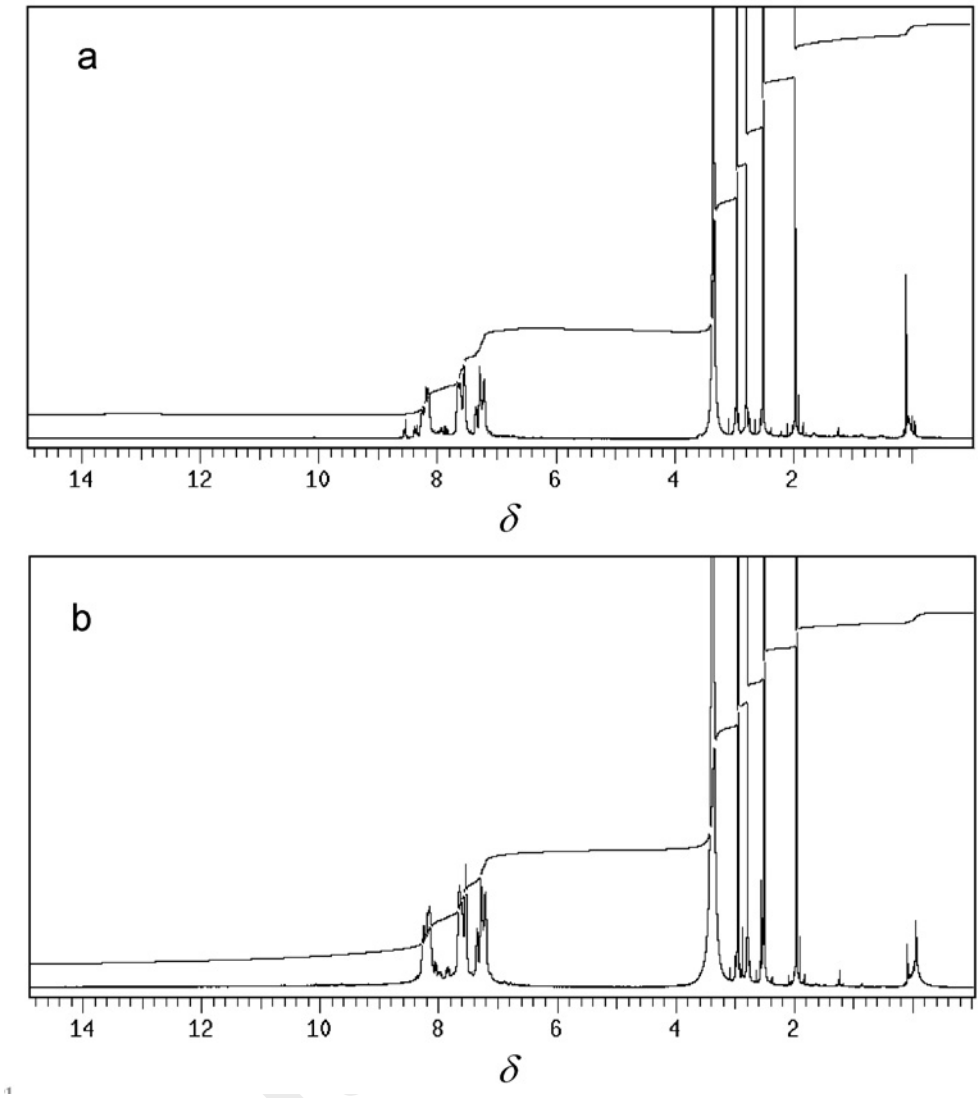

Fig. 6. ^{1}H NMR spectrum of PI–zeolite–5.2 mass % PDMS 1000 g mol^{-1} (a) and PI–zeolite-5.2 mass % PDMS 3200 g mol^{-1} (b).

The decrease in the volume fraction of the filler means that the amino-terminated PDMS participates in the polymerisation. When the volume fraction of the filler started to increase (addition of 5.2 mass % PDMS (3200 g mol^{-1})) the value of φ decreased to 0.06 (Table 1), this means that the PDMS was adsorbed on the zeolite surface rather than forming inclusions in the zeolite pores. In the case of the addition of 3.2 mass % PDMS (3200 g mol^{-1}), the value of φ was 0.16 (Table 1), i.e. nanocrystallisation contributed to the increment of volume fraction of the filler.

The pristine PI and the zeolite-filled PI exhibited the highest transparency (Fig. 7, spectra A and B). The hybrid PI–zeolite–3.2 mass % PDMS (1000 g mol^{-1}) material exhibited good transparency with 70 % transmittance at 750 nm. The incorporation of PDMS of above 3.2 mass % and both 3.2 mass % and 5.2 mass % PDMS (3200 g mol^{-1}) decreased the transparency. The SEM images of PDMS-containing materials presenting spherical, porous phases in the smooth PI and PI–zeolite matrix (Figs. 8f and 8h) became opaque (Fig. 7, spectra D–F). The porous phases could correspond to PDMS due to the appearance when PDMS of 5.2 mass % was used (Figs. 8f and 8h). The phase separation took place at microscale -when PDMS of 5.2 mass % -was applied. The interfacial attraction between two phases such as PI–zeolite, PI–PDMS, zeolite–PDMS affects the transparency. The findings relating to the volume fraction of the filler (Table 1) influenced the optical transparency. The lower the volume fraction of the filler, φ of 0.05 for 5.2 mass % PDMS (1000 g mol^{-1} (Table 1), the more opaque the material. This is because the inclusion of silicone, present in PI-zeolite in a high amount (Fig. 7, spectrum D), decreases the intensity of light passing through zeolite. The increase in the volume fraction of the filler (addition of 5.2 mass % PDMS (3200 g mol^{-1})), resulting in φ value of 0.06 (Table 1), led to lower sample transparency (Fig. 7, spectrum F), despite the silicone adsorbed on the zeolite sur-

Table 1. Volume fraction of filler (φ) determined by Guth equation (Eq. (2)) depending on storage moduli (E') at a certain temperature (75 °C)

Sample	Storage modulus, MPa	Volume fraction of the filler
PI	369	–
PI–zeolite	1134	0.31
PI–zeolite–3.2 mass % PDMS (1000 g mol^{-1})	539	0.11
PI–zeolite–5.2 mass % PDMS (1000 g mol^{-1})	428	0.05
PI–zeolite–3.2 mass % PDMS (3200 g mol^{-1})	650	0.16
PI–zeolite–5.2 mass % PDMS (3200 g mol^{-1})	435	0.06

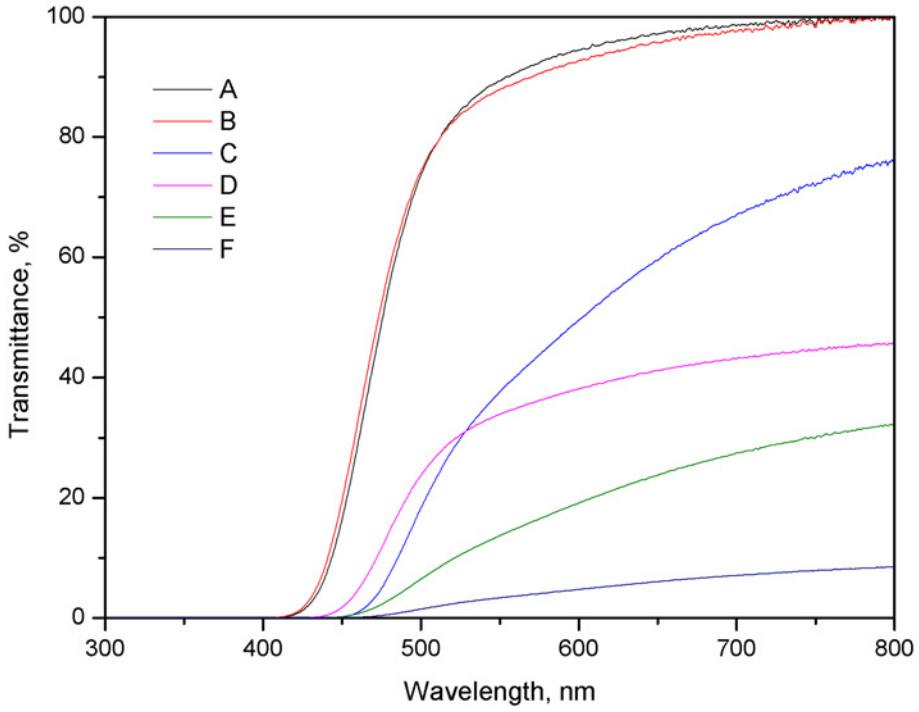

Fig. 7. UV-VIS spectra of material: PI (A), PI–zeolite (B), PI–zeolite–3.2 mass % PDMS (1000 g mol^{-1}) (C), PI–zeolite–5.2 mass % PDMS (1000 g mol^{-1}) (D), PI–zeolite–3.2 mass % PDMS (3200 g mol^{-1}) (E), and PI–zeolite–5.2 mass % PDMS (3200 g mol^{-1}) (F).

face. This can be explained by the fact that the zeolite transmits light, while light-scattering (translucency) takes place in the case of silicone. In comparing the materials in Fig, 7, spectra D and F, the silicone-surrounded zeolite content confirmed by the diminished alkyl vibration (Fig. 4, spectrum F) caused more opaque material than the material comprising the silicone-included zeolite.

The PI–zeolite–3.2 mass % PDMS (3200 g mol^{-1}) (Fig. 8g) mostly represented the pore-filled structure despite the high molecular mass-silicone ingredient. Here, XRD pattern nanocrystallite phases (Fig. 9, points a and b) appeared in the sample. A crystalline zeolite layer in the amorphous phase was identified by the Bragg-reflected characteristic peaks of zeolite Y from XRD. Faujasite (compared with those in powder pattern identification table), FAU[111] (2θ = 6.18°, I% = 100, b = 0.209°, XS = 434 Å) and FAU[555] (2θ = 31.38°, I % = 52, b = 0.213°, XS = 438 Å) was observed. Using the Scherrer equation (Eq. (1)), D_p (crystallite size) were calculated as 382 Å and 437 Å, respectively. The pore-filled structure of the PI–zeolite–3.2 mass % PDMS (3200 g mol^{-1}) is due to the nanocrystallite formation.

The MMMs exhibited a hydrophobic surface (Table 2). The hydrophobicity increased from 86° to 92° with the introduction of modified zeolite. This result and also the SEM image confirmed the successful covalent bond formation between the polymer and zeolite. The hydrophobic silica-rich zeolite increased the contact angle value. However, the hydrophobicity and also the porosity continued to increase with the addition of PDMS (Table 2). Special interest was directed towards the patterned wettability within the complex microchannel networks shown by Schneider (2011), as it is of major interest to the petroleum industry to inves-

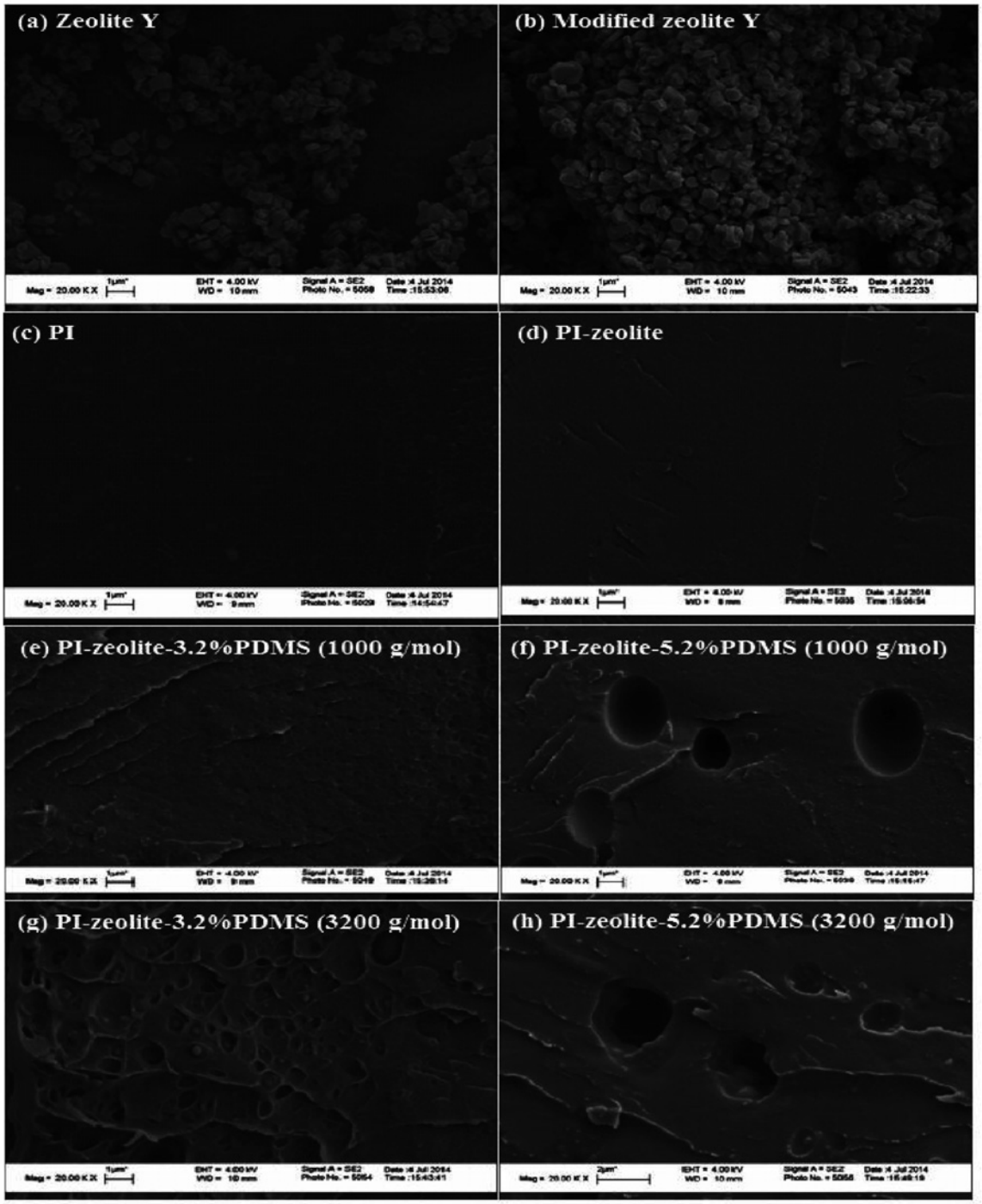

Fig. 8. SEM images of materials: zeolite Y (a), modified zeolite Y (b), PI (c), PI–zeolite (d), PI–zeolite–3.2 mass % PDMS (1000 g mol^{-1}) (e), PI–zeolite–5.2 mass % PDMS (1000 g mol^{-1}) (f), PI–zeolite–3.2 mass % PDMS (3200 g mol^{-1}) (g), and PI–zeolite–5.2 mass % PDMS (3200 g mol^{-1}) (h).

tigate the multiphase flow properties in porous media of heterogeneous wettability with the aid of such systems. Some aspects of the above study are beyond the scope of this work, but the heterogeneity of a solid surface, the roughness and wettability within channel networks may be taken into account. For clarity, the presence of a hydrophobic poly(dimethylsiloxane) moiety in the present study created an inverse relationship between the porosity of the materials (surface roughness) and the hydrophilicity (wettability). Khung et al. (2007) reported that surface silanisation with PEGS and APTES created hydrophilic surfaces which made it possible for the water droplets to penetrate the pores. In this way, the decrease in contact angles was observed from the large pores to the small pores, and the hydrophilicity increased. Rogers

Table 2. Contact angles, thermal gravimetric analyses (TGA) and glass transition temperature (T_g) results, and tensile properties of materials

Sample	Contact angle	Mass loss temperature T_d, ℃		Char	Glass transition temperature, T_g, ℃		Modulus	Strength	Elongation at break
	θ, °	first	second	%	first	second	GPa	MPa	%
PI	86	252	475	44	–	322	2.22 ± 0.1	17 ± 1	10 ± 1
PI–zeolite	92	267	505	48	–	307	2.91 ± 0.1	23 ± 1	13 ± 1
PI–zeolite–3.2 mass % PDMS (1000 g mol^{-1})	98	270	530	49	–	280	2.28 ± 0.1	32 ± 1	14 ± 1
PI–zeolite–5.2 mass % PDMS (1000 g mol^{-1})	100	270	532	51	213	274	1.88 ± 0.1	20 ± 1	15 ± 1
PI–zeolite–3.2 mass % PDMS (3200 g mol^{-1})	104	287	535	53	–	202[a]	2.15 ± 0.1	27 ± 1	18 ± 1
PI–zeolite–5.2 mass % PDMS (3200 g mol^{-1})	110	322	553	53	190	238	1.24 ± 0.1	21 ± 1	24 ± 1

a) Crystallisation temperature (T_c, exotherm peak).

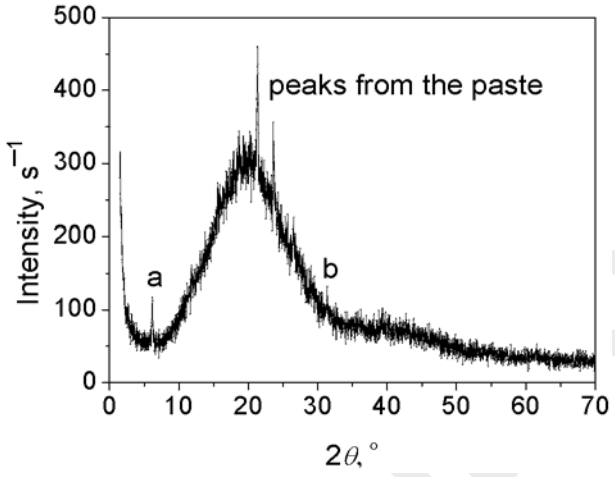

Fig. 9. XRD pattern of PI–zeolite–3.2 mass % PDMS (3200 g mol^{-1}): 2θ = 6.18°, d = 14.29 Å, (full width at half maximum, FWHM) b = 0.209°, (crystallite size) XS = 434 Å (a); 2θ = 31.38°, d = 2.85 Å, (FWHM) b = 0.213°, (crystallite size) XS = 438 Å (b).

et al. (2005) indicated that, for polymers capable of hydrogen bonding, such as polyamides, the use of an organophilic coating on the clay was sufficient to initiate successful intercalation and subsequent exfoliation of the clay within the matrix. It is assumed that there could be an inverse relationship between hydrophilicity and surface roughness. It is probable that the zeolite-filled polyimide porous structures could be surrounded by PDMS which is hydrophobic. The presence of hydrophobic moieties around the polyimide matrix could impede penetration of the water droplets into the pores so that the hydrophobicity increased. The high molecular mass PDMS (3200 g mol^{-1}) in a high amount decreased the intensity of the peak related to the CH_3—Si protons in the δ region from –0.10 to 0.05 (Fig. 6b), as reported by Nakagawa et al. (2002). The PI–zeolite–5.2 % PDMS (1000 g mol^{-1}) material displayed a sharp singlet peak (CH_3—Si protons, Fig. 6a) in δ region from –0.10 to 0.05, while the PI–zeolite–5.2 % PDMS (3200 g mol^{-1}) material presented a doublet peak with the decreased intensity (CH_3—Si protons, Fig. 6b). This result suggests that 5.2 mass % PDMS (3200 g mol^{-1}) surrounded the PI–zeolite through a non-covalent interaction between the silicone NH_2 proton and the carbonyl oxygen of the zeolite–polyimide instead of pore-filling. Accordingly, the hydrophobicity was increased. The increased hydrophobicity for 3.2 mass % PDMS (3200 g mol^{-1}) is explained by the nanocrystalline zeolite layer in the amorphous region.

Thermal and mechanical properties

The first decomposition temperatures indicated the removal of the solvent trapped by zeolite. The thermal stability of the materials was improved with the increase in PDMS content (Table 2, Fig. 10).

The incorporation of the PDMS improved the elongation at break. The tensile modulus and strength, measured at ambient temperature, of the zeolite containing PI (Table 2) was greater than that of the neat PI. This result indicated that polymerisation proceeded in the zeolite pores. The polymerisation that occurred in the pores of the MSNs (mesoporous silica nanocomposite)-doped PI was previously reported as explaining the improvement in mechanical properties by Ye et al. (2014). The addition of 3.2 mass % of silicone (1000 g mol^{-1}) improved the tensile strength and elongation at break as compared with those of the neat PI (Table 2), meaning that the amino groups of PDMS reacted with the polyamic acid–zeolite filling the pores. The storage modulus (E') obtained from the temperature-dependent DMA (Fig. 10, TGA curve B) of the PI–zeolite was greater than that of PI (Fig. 10, curve A), which again clearly indicated that polymerisation had occurred in the zeolite pores. The

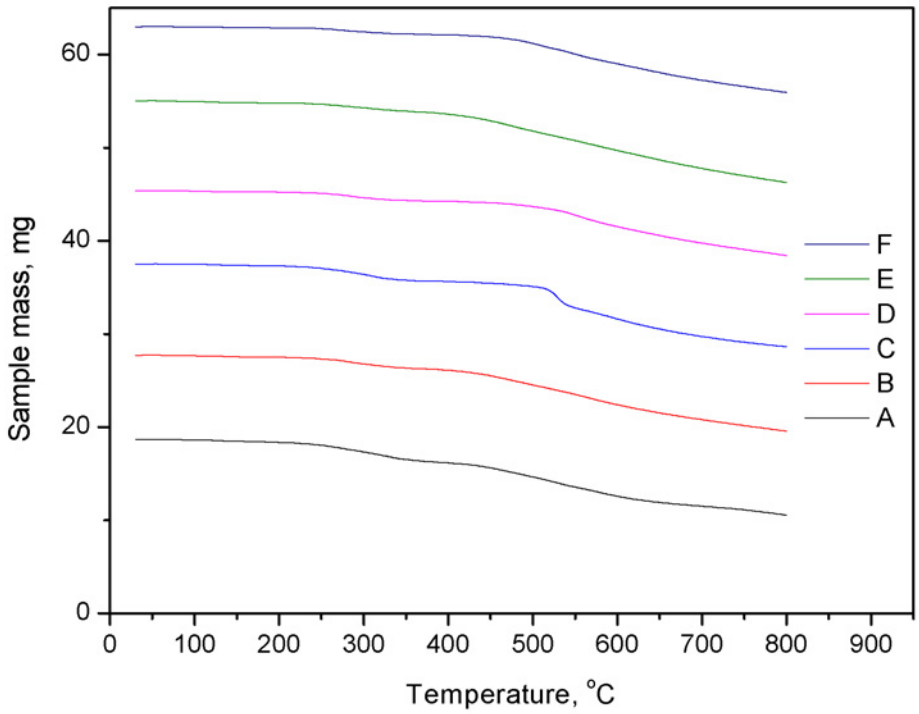

Fig. 10. Thermogravimetric analysis (TGA) results for material: PI (A), PI–zeolite (B), PI–zeolite–3.2 mass % PDMS (1000 g mol^{-1}) (C), PI–zeolite–5.2 mass % PDMS (1000 g mol^{-1}) (D), PI–zeolite–3.2 mass % PDMS (3200 g mol^{-1}) (E), and PI–zeolite–5.2 mass % PDMS (3200 g mol^{-1}) (F).

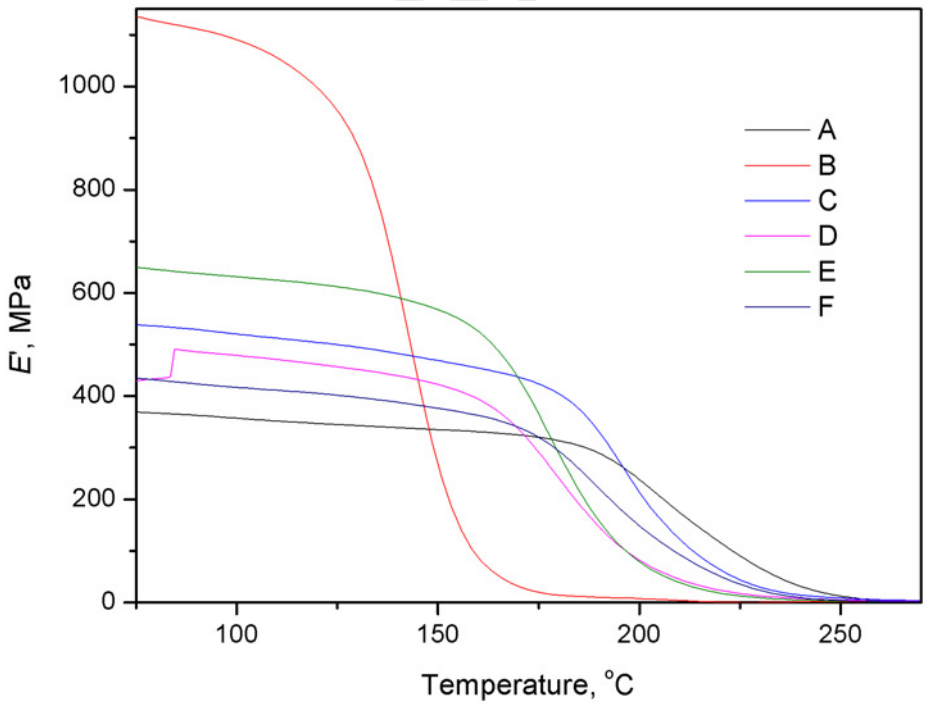

Fig. 11. Temperature-dependent storage moduli obtained from DMA of material: PI (A), PI–zeolite (B), PI–zeolite–3.2 mass % PDMS (1000 g mol^{-1}) (C), PI–zeolite–5.2 mass % PDMS (1000 g mol^{-1}) (D), PI–zeolite–3.2 mass % PDMS (3200 g mol^{-1}) (E), and PI–zeolite–5.2 mass % PDMS (3200 g mol^{-1}) (F).

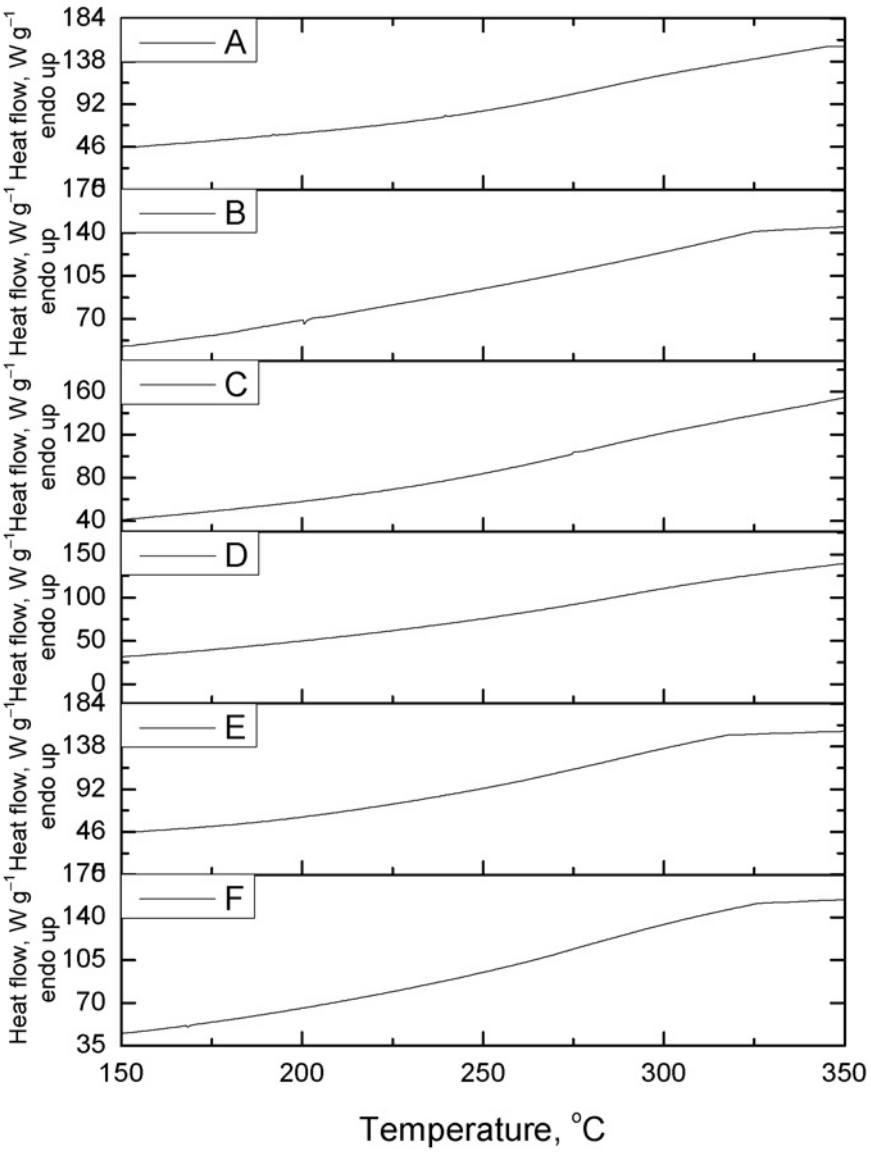

Fig. 12. Glass transition temperatures deduced from DSC curves for material: PI–zeolite–5.2 mass % PDMS (3200 g mol^{-1}) (A), PI–zeolite–3.2 mass % PDMS (3200 g mol^{-1}) (B), PI–zeolite–5.2 mass % PDMS (1000 g mol^{-1}) (C), PI–zeolite–3.2 mass % PDMS (1000 g mol^{-1}) (D), PI–zeolite (E), and PI (F).

addition of flexible PDMS (3.2 mass %, 1000 g mol^{-1}) gave rise to an increase in the tensile modulus of the neat PI. In comparison with the storage modulus of PI, the 3.2 mass % PDMS (1000 g mol^{-1}) also improved the storage modulus (Fig. 11, curve C). When the amount of silicone increased in the presence of 5.2 mass % PDMS (1000 g mol^{-1}), the tensile modulus, strength (Table 2), and the storage modulus (Fig. 11, curve D) decreased. When comparing the materials containing low molecular mass PDMS (1000 g mol^{-1}), the storage modulus (Fig. 11, curve E), tensile modulus, strength, and elongation at break (Table 2) increased with increasing the molecular mass of silicone (3.2 mass %, 3200 g mol^{-1}) due to the reinforcing effect of the nanocrystalline formation (Fig. 9, points a and b). The highest content (5.2 mass %) of the highest molecular mass silicone (3200 g mol^{-1}) caused a decrease in the tensile modulus, strength (Table 2), and the storage modulus (Fig. 11, curve F) compared with those of the same molecular mass silicone (3200 g mol^{-1}) but present in the lowest amount (3.2 mass %) (Fig. 11, curve E). However, the elongation at the break of the PI–zeolite–5.2 mass % PDMS (3200 g mol^{-1}) was greater than that of the PI–zeolite–3.2 mass % PDMS (3200 g mol^{-1}). This result is attributed to the PDMS surrounding the PI–zeolite. Taking into consideration the 1 % and 5 % difference in elongation at the break values for the samples doped with the lowest molecular mass and highest molecular mass silicone in different amounts, respectively, it is

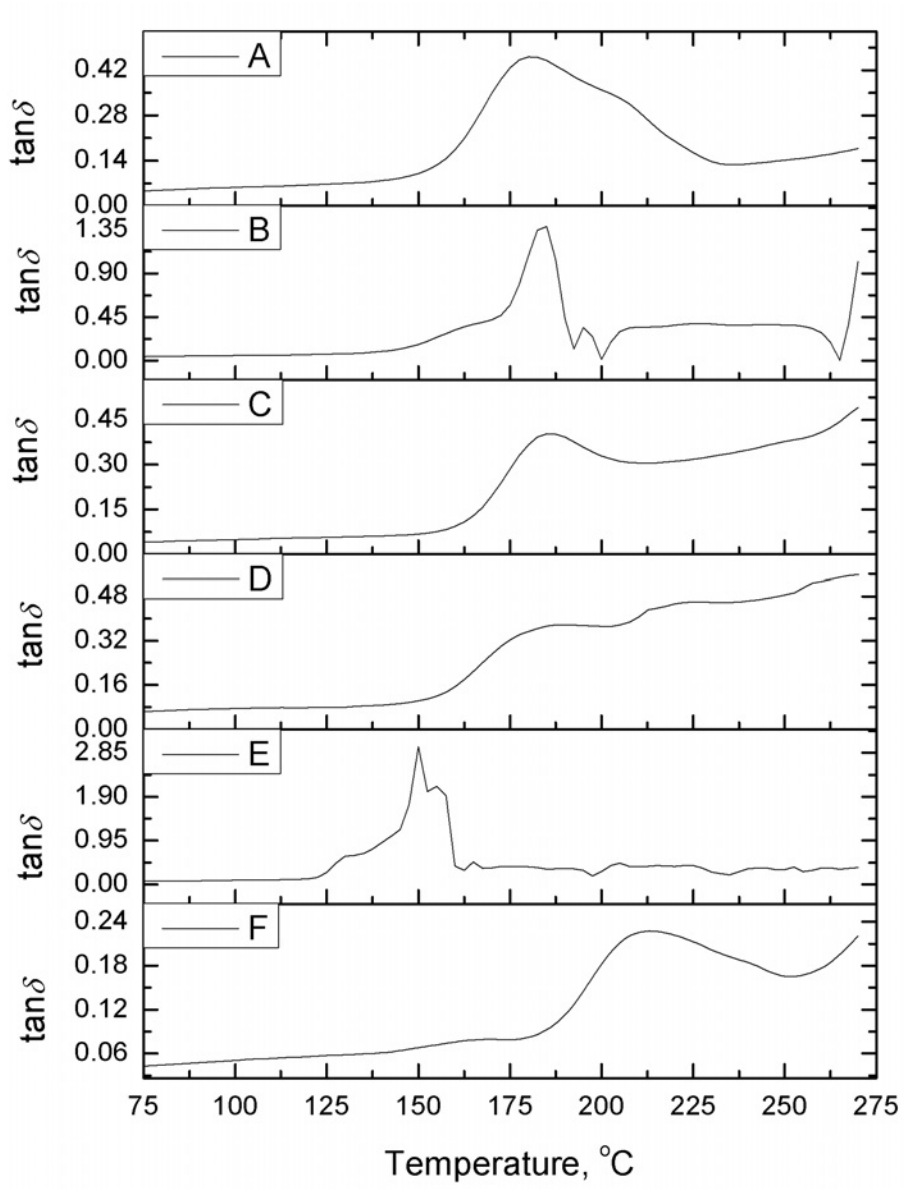

Fig. 13. Glass transition temperatures deduced from DMA for material: PI–zeolite–5.2 mass % PDMS (3200 g mol^{-1}) (A), PI–zeolite–3.2 mass % PDMS (3200 g mol^{-1}) (B), PI–zeolite–5.2 mass % PDMS (1000 g mol^{-1}) (C), PI–zeolite–3.2 mass % PDMS (1000 g mol^{-1}) (D), PI–zeolite (E), and PI (F).

clear that 3200 g mol^{-1} silicone surrounded the PI–zeolite being adsorbed on the zeolite surface.

The glass transition temperatures (T_g) of the materials decreased, starting from the neat PI up to the PI–zeolite–3.2 mass % PDMS (1000 g mol^{-1}) (Table 2, Figs. 12, curves D–F, Figs. 13, curves D–F). The introduction of zeolite led to free volume enhancement and the addition of flexible silicone decreased glass transition temperatures. The two glass transition temperatures (T_g, Fig. 12) derive from two phases such as PI–zeolite, PI–PDMS, or zeolite–PDMS. The glass transition temperature decreased, attaining a specific filler volume fraction of φ 0.11, for the sample doped with 3.2 mass % PDMS (1000 g mol^{-1}) (Table 1). The addition of 3.2 mass % PDMS (3200 g mol^{-1}) resulted in an exotherm peak seen in the DSC curve (Fig. 12, curve B). This exotherm peak was clearly identified in the DMA curve (Fig. 13, curve B). The exotherm peak is attributed to the crystallisation temperature (T_c) of the PI–zeolite–3.2 mass % PDMS (3200 g mol^{-1}). The crystallisation leading to more free volume resulted in a decreased glass transition temperature (Fig. 13, curve B). The increment of the glass transition temperature of the material containing 5.2 mass % PDMS (3200 g mol^{-1}) compared to that containing 3.2 mass % PDMS (3200 g mol^{-1}) (Fig. 13) points to polymer-chain rigidification caused by silicone adsorbed on the zeolite surface.

Conclusions

The use of faujasite-type zeolites alone may cause brittle structures. Before considering zeolites as candidates in various fields in future, adequate properties should be achieved by blending them with appropriate polymers in the due amounts. In this study, the thermal stability of the materials increased as the PDMS content increased. To understand the changes in tensile properties, the storage moduli the polymerisation pathway such as pore-filling mechanism or being surrounded by other polymers should be taken into consideration. The pore-filling as seen in the PI–zeolite, improved the mechanical property. The nanocrystallite layer providing a reinforcing effect, identified by XRD, DMA, the DSC crystallisation peak, in the amorphous region of PI–zeolite–3.2 mass % PDMS (3200 g mol^{-1}) improved the storage modulus. The amino groups of PDMS-1000 g mol^{-1} in either 3.2 mass % or 5.2 mass % reacted with the polyamic acid–zeolite filling the pores, however the PDMS-3200 g mol^{-1} of 5.2 mass % reacted physically with the zeolite being adsorbed onto the zeolite surface. Despite the flexibility of 3.2 mass % of the silicone (1000 g mol^{-1}) content, the enhanced tensile modulus and storage modulus could be explained by the fact that the silicone rearranges PI orientation due to pore-filling. The 5.2 mass % of PDMS with the molecular mass of 3200 g mol^{-1} in this study may be regarded as an organophilic coating material on the zeolite due to the decline in the intensity of the alkyl stretching and the marked difference in elongation at break values of PI–zeolite–3.2 mass % PDMS (3200 g mol^{-1}) and PI–zeolite–5.2 mass % PDMS (3200 g mol^{-1}) compared with those of other PDMS-containing materials. This organophilic-coating moiety inversely affected the hydrophilicity.

Acknowledgements. This work was supported by Marmara University project no. BAPKO-FEN-E-090113-0006. The NMR, SEM, and DMA measurements were performed at the Faculty of Natural Science and Engineering, Sabancı University. The PSA and XRD measurements were performed at the R&D Centre, Boğaziçi University.

References

Alam, S. M. M., Agag, T., Kawauchi, T., & Takeichi, T. (2007). Organic–inorganic hybrids containing polyimide, organically modified clay and in situ formed polydimethylsiloxane. *Reactive and Functional Polymers*, *67*, 1218–1224. DOI: 10.1016/j.reactfunctpolym.2007.07.003.

Freeman, B. D. (1999). Basis of permeability/selectivity tradeoff relations in polymeric gas separation membranes. *Macromolecules*, *32*, 375–380. DOI: 10.1021/ma9814548.

Güngör, A., Smith, C. D., Wescott, J., Srinivasan, S., & McGrath, J. E. (1991). Synthesis of fully imidized phosphorous-containing soluble polyimides. *ACS Polymer Preprints*, *32*, 172–173.

Guth, E. (1945). Theory of filler reinforcement. *Journal of Applied Physics*, *16*, 20–25. DOI: 10.1063/1.1707495.

Khung, Y. L., Cole, M. A., McInnes, S. J. P., & Voelcker, N. H. (2007). Control over wettability via surface modification of porous gradients. In D. V. Nicolau, D. Abbott, K. Kalantar-Zadeh, T. Di Matteo, & S. M. Bezrukov (Eds.) *Proceedings of SPIE*, (Vol. *6799*, 679909). DOI: 10.1117/12.759377.

Kickelbick, G. (2003). Concepts for the incorporation of inorganic building blocks into organic polymers on a nanoscale. *Progress in Polymer Science*, *28*, 83–114. DOI: 10.1016/s0079-6700(02)00019-9.

Kricheldorf, H. R. (Ed.) (1996). *Silicon in polymer synthesis.* Berlin, Germany: Springer. DOI: 10.1007/978-3-642-79175-8.

Nakagawa, T., Nishimura, T., & Higuchi, A. (2002). Morphology and gas permeability in copolyimides containing polydimethylsiloxane block. *Journal of Membrane Science*, *206*, 149–163. DOI: 10.1016/s0376-7388(01)00775-x.

Nakata, S., Kawata, M., Kakimoto, M. A., & Imai, Y. (1993). Synthesis and properties of new block copolymers based on polydimethylsiloxane and tetraphenylethylene-containing polyimide. *Journal of Polymer Science Part A: Polymer Chemistry*, *31*, 3425–3432. DOI: 10.1002/pola.1993.080311331.

Rogers, K., Takacs, E., & Thompson, M. R. (2005). Contact angle measurement of select compatibilizers for polymer-silicate layer nanocomposites. *Polymer Testing*, *24*, 423–427. DOI: 10.1016/j.polymertesting.2005.01.010.

Sang, S. Y., Liu, Z. M., Tian, P., Liu, Z. Y., Qu, L. H., & Zhang, Y. Y. (2006). Synthesis of small crystals zeolite NaY. *Materials Letters*, *60*, 1131–1133. DOI: 10.1016/j.matlet.2005.10.110.

Schneider, M. (2011). *Wettability patterning in microfluidic systems and applications in the petroleum industry.* Ph.D. thesis, Pierre and Marie Curie University, Paris, France.

Steed, J. W., & Atwood, J. L. (2009). *Supramolecular chemistry* (2nd ed.). Chichester, UK: Wiley.

Te Hennepe, H. J. C., Bargeman, D., Mulder, M. H. V., & Smolders, C. A. (1987). Zeolite-filled silicone rubber membranes: Part 1. Membrane preparation and pervaporation results. *Journal of Membrane Science*, *35*, 39–55. DOI: 10.1016/s0376-7388(00)80921-7.

Ye, X. Y., Wang, J. Q., Xu, Y., Niu, L. Y., Fan, Z. J., Gong, P. W., Ma, L. M., Wang, H. G., Yang, Z. G., & Yang, S. R. (2014). Mechanical properties and thermostability of polyimide/mesoporous silica nanocomposite via effectively using the pores. *Journal of Applied Polymer Science*, *131*, 41173. DOI: 10.1002/app.41173.

Zuo, M., Takeichi, T., Matsumoto, A., & Tsutsumi, K. (1998). Surface characterization of polyimide films. *Colloid Polymer Science*, *276*, 555–564. DOI: 10.1007/s003960050281.